Supporting Information

Voltage induced electrochemical reactions of single lithium-rich layer-oxide

nanoparticles

Tao Li, Bohang Song, Li Lu and Kaiyang Zeng*

Department of Mechanical Engineering

National University of Singapore

Engineering Drive 1, Singapore 117576

* Corresponding author, E-mail: mpezk@nus.edu.sg

Figure S1, (a) X-ray diffraction (XRD) pattern of pristine LR nanoparticles. It demonstrates the presents of both LMO and NCM phases.[1] The majority of particles were oriented in $(003)_R(001)_M$ and $(104)_R(202)_M$ planes. R represents layered monoclinic structure, and M represents layered rhombohedral structure. (b) Charging/discharging curves that show the featured capacity loss of LR nanoparticle during the first cycle.
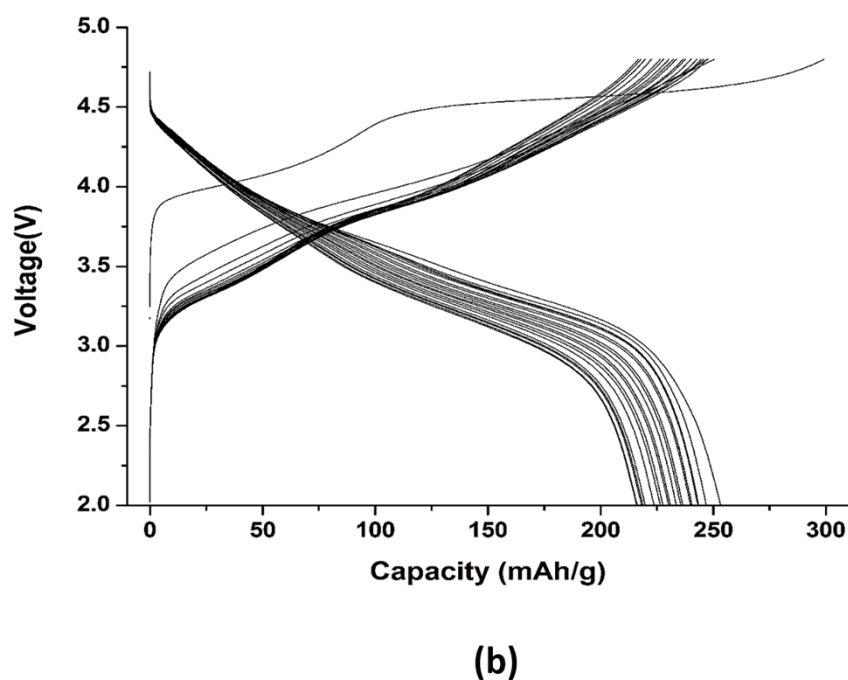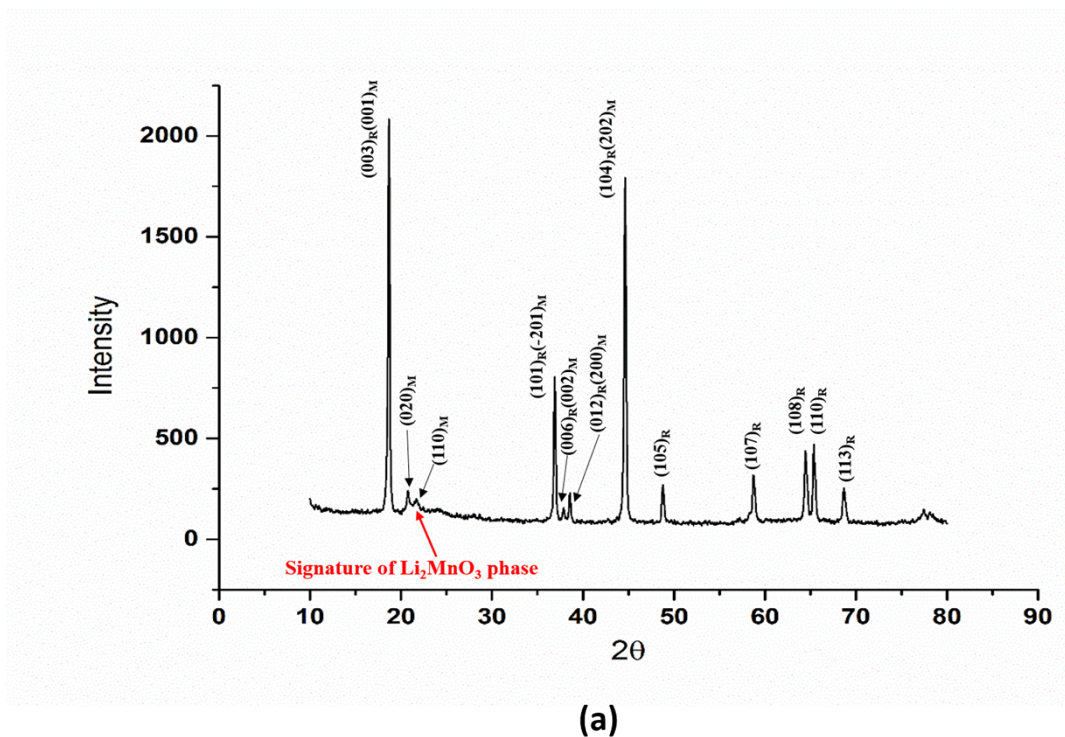

(a)

(b)

Table S1, Averaged ratio of reduced elastic modulus between LMO and NCM nanoparticles. The stiffness of Pt-substrate was used as a reference because it should be the same regardless of different image and tip condition. The contact stiffness ratios of individual particle with respect to the correspondence Pt-substrate are summarized in Table 1a. According to Hertzian contact model, $E/E_{Pt} = (k^c/k^c_{Pt})^m$, where m=3/2, and "E" is the reduced elastic modulus of the tip-sample system.[2]

$$\frac{1}{E} = \frac{1 - \upsilon_{tip}^{2}}{E_{tip}} + \frac{1 - \upsilon_{sample}^{2}}{E_{sample}}$$

(S1)

The particle and Pt-substrate were scanned with the identical tip conditions. Thus, the first term in the equation is always the same constant.

The ratios of E among Pt, NCM and LMO are listed in Table 1b.

Particle Number		Contact stiffness, k^c (mN/m)					
	NCM	Pt_{NCM}	k^c_{Pt}/k^c_{NCM}	LMO	Pt_{LMO}	k^c_{Pt}/k^c_{LMO}
1	358.67	503.45	1.40	355.41	475.49	1.34
2	366.70	497.23	1.36	376.78	477.57	1.27
3	376.60	496.58	1.32	409.69	478.74	1.17
4	384.79	496.13	1.29	413.69	477.97	1.16
5	388.20	502.63	1.29	466.75	472.10	1.01
6	411.67	497.68	1.21	470.61	474.76	1.01
7	416.02	499.52	1.20	418.92	466.58	1.11
8	471.05	539.49	1.15	431.27	496.99	1.15
average			1.30±0.07			1.15±0.11

Table 1a

Materials	Ratio of reduced E
E_{Pt}/E_{LMO}	1.23
E_{Pt}/E_{NCM}	1.48
E_{LMO}/E_{NCM}	1.20

Table 1b

Figure S2, Stiffness variations of the Pt-substrate after applying long-hold voltage to LR particle. The contact stiffness $k^c=2aE$, where "a" is the contact radius. For Pt-substrate, whose E should be a constant value so that the k^c is proportional to the contact radius a, which is affected by loading force and radius of curvature of the tip. If tip is perfectly stable, k^c should also be a constant value.

However, it is found that k^c of Pt-substrate increases linearly from 0 to 4 V, which clearly indicates the continuous change of contact radius that is originated from systematic tip wear. At voltages higher than 4.5 V, the dramatic change of k^c should be mainly due to the EC reaction of the nanoparticle, in which case the Pt-substrate can be affected. Therefore, the stiffness images (0 to 4.5 V) in **Fig.2** (main text) were corrected by multiplying a factor to maintain a constant k^c for Pt-substrate.
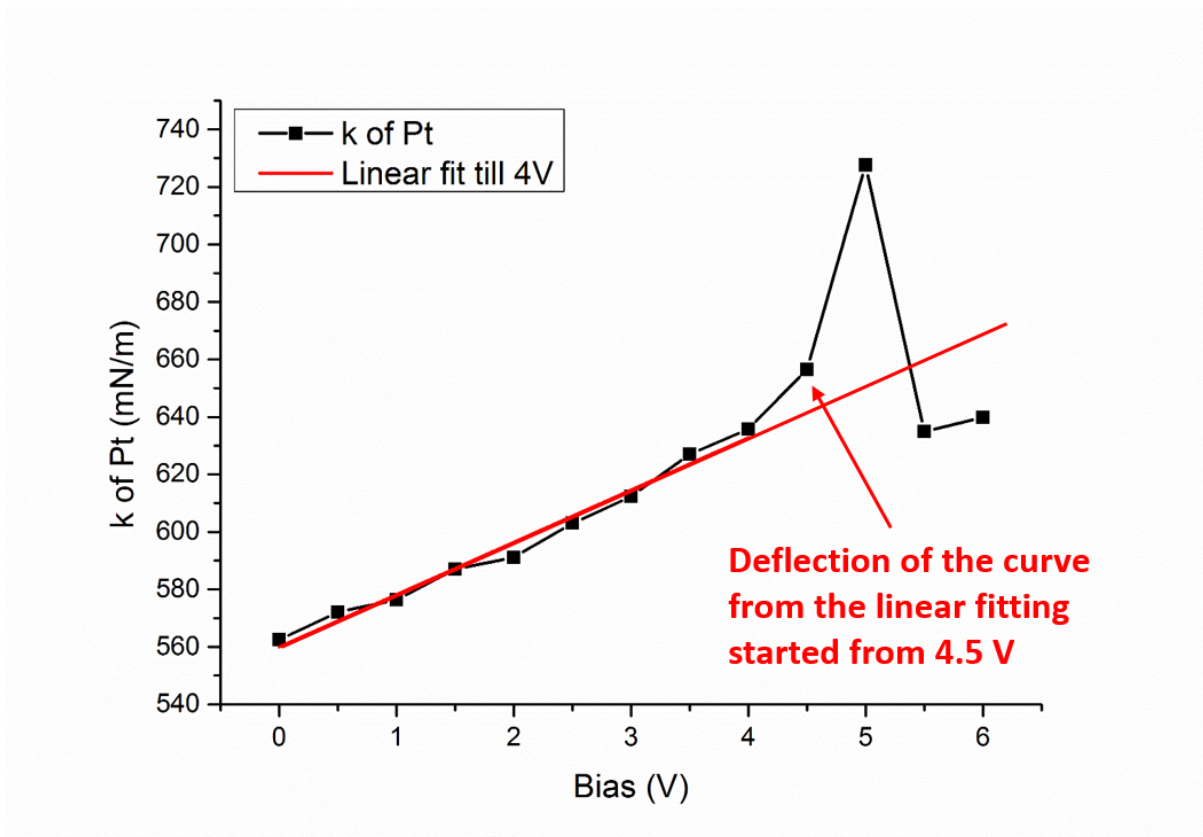
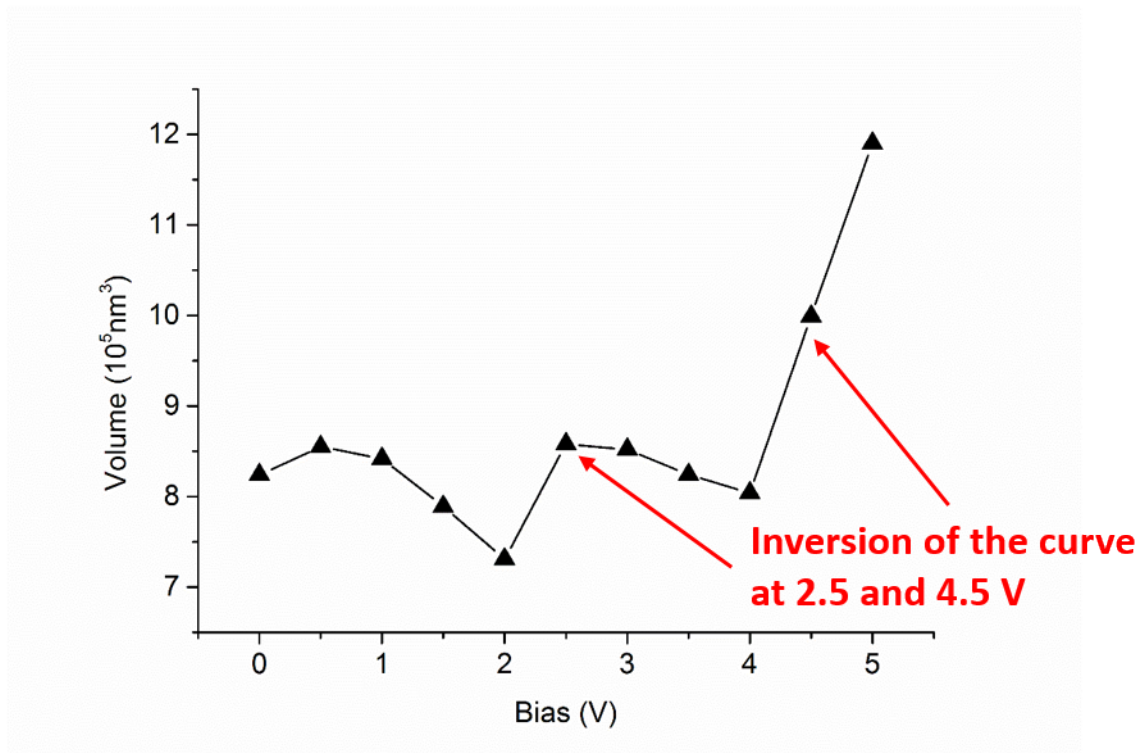Figure S3, Volume evolution of LR nanoparticle induced by long-hold positive voltages in AA.

Figure S4, Bimodal-AM imaging of NCM in AA. Particle was scanned under repulsive regime with scan size of $1 \times 1 \ \mu m^2$. Long-hold voltages were applied in the middle of particle surface from 0 to 6 V with 1 V increment. As explained in the main text section, Bimodal-AM A2 image has the inverted contrast to that of the AM-FM stiffness image. Thus, higher A2 value corresponds to the lower stiffness. As pointed by the arrows, new materials were formed at the location where 5 V and 6 V biases was applied.

For this particle, upon increasing positive voltages, more and more new materials with lower stiffness gradually formed at the tip-sample contact region that may be due to the cation metal reduction. Some other particles show dimples form at the particle surface, which may be due to the decreased lattice volume caused by locally increased concentration of Li^+-ions in the layered-structure.

It is found that bias induced Li^+-ion movement in NCM is highly directional dependent, preferred along the Li-layer and impeded perpendicular to the Li-layer. Depending on the location of applied bias (electric field is parallel or perpendicular to Li-layer), NCM nanoparticle can be locally expanded, contracted, fractured, or form new materials. It seems that this anisotropic characteristic does not show in LR nanoparticles. The volume of the NCM nanoparticle also remains constant below 4 V, rather than in a cyclic pattern as that of LR particle (Fig.S3).
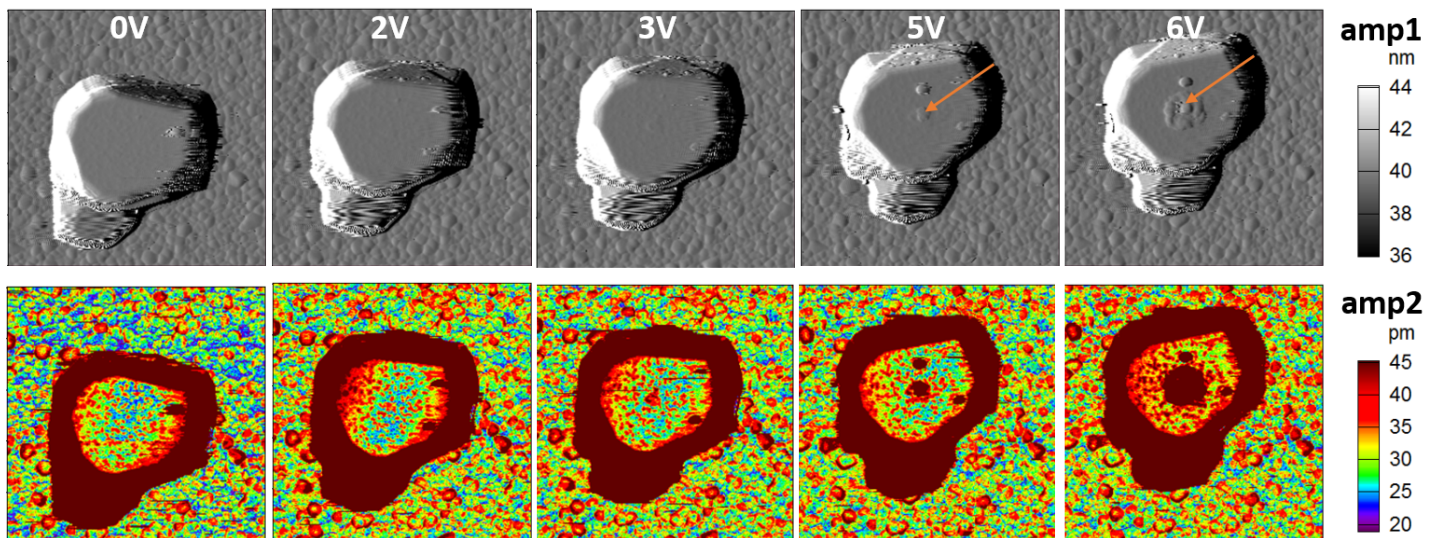
Figure S5, Bimodal-AM imaging of LMO in AA. Particle was scanned under repulsive regime with scan size of 2×2 μm². Biases were applied at the red marked place from 0 to 8 V with 1 V increment. Nearly no morphology change is observed and local stiffness and compositional variations are also minor, and this indicates the EC inert characteristic of pure LMO.
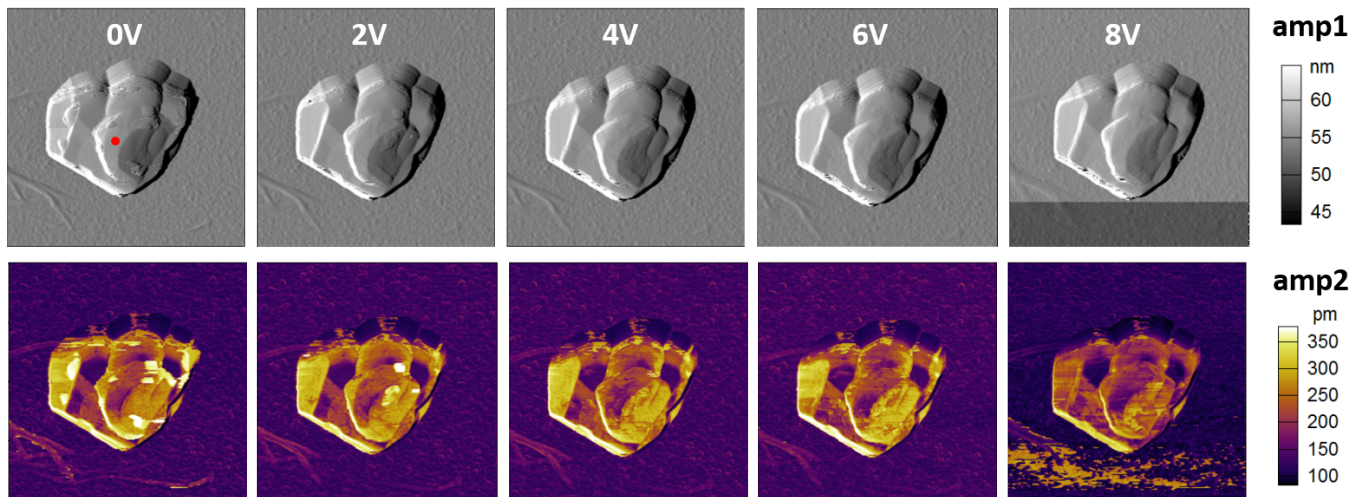
Figure S6, Amplitude2 (A2) and phase2 of Pt-substrate versus voltage in SA (attractive regime) (a), and Ar (repulsive regime) (b) that observed by Bimodal-AM. The tip wear causes the measured parameters of Pt-substrate change continuously.

At low voltages, the changes of A2 and phase2 are gradual and linear. When applied bias is higher than 4 V, sudden dramatic property change of Pt-substrate are usually observed, in which may not be caused by tip blunting. This makes the speculation that Pt substrate may be affected by or involved in certain reactions with the LR particle with unknown mechanism. It may have certain implications on the reactions between active electrode and current collector.

In addition, depending on the first eigenmode regimes, A2 and phase2 show either similar (in repulsive regime) or inverse (in attractive regime) trend and contrast. This observation further described the responsive behaviors of Bimodal-AM technique.
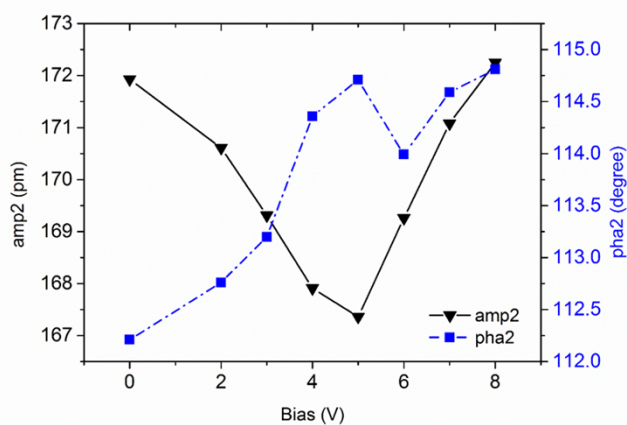
a
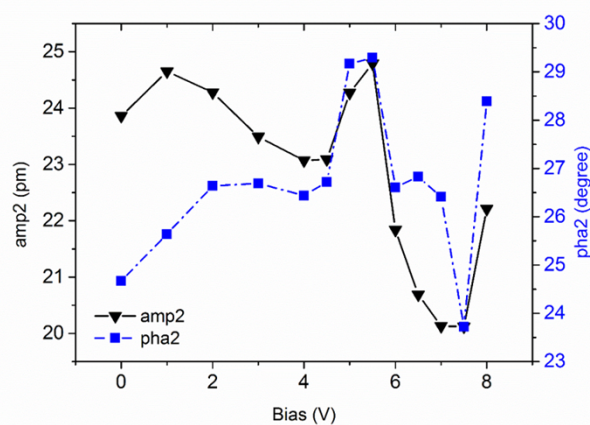
b

Figure S7, Bimodal-AM images of LR nanoparticle in SA. Negative voltages (-2 to -7 V) are applied at the center of the particle surface. Image size is 350 × 350 nm².
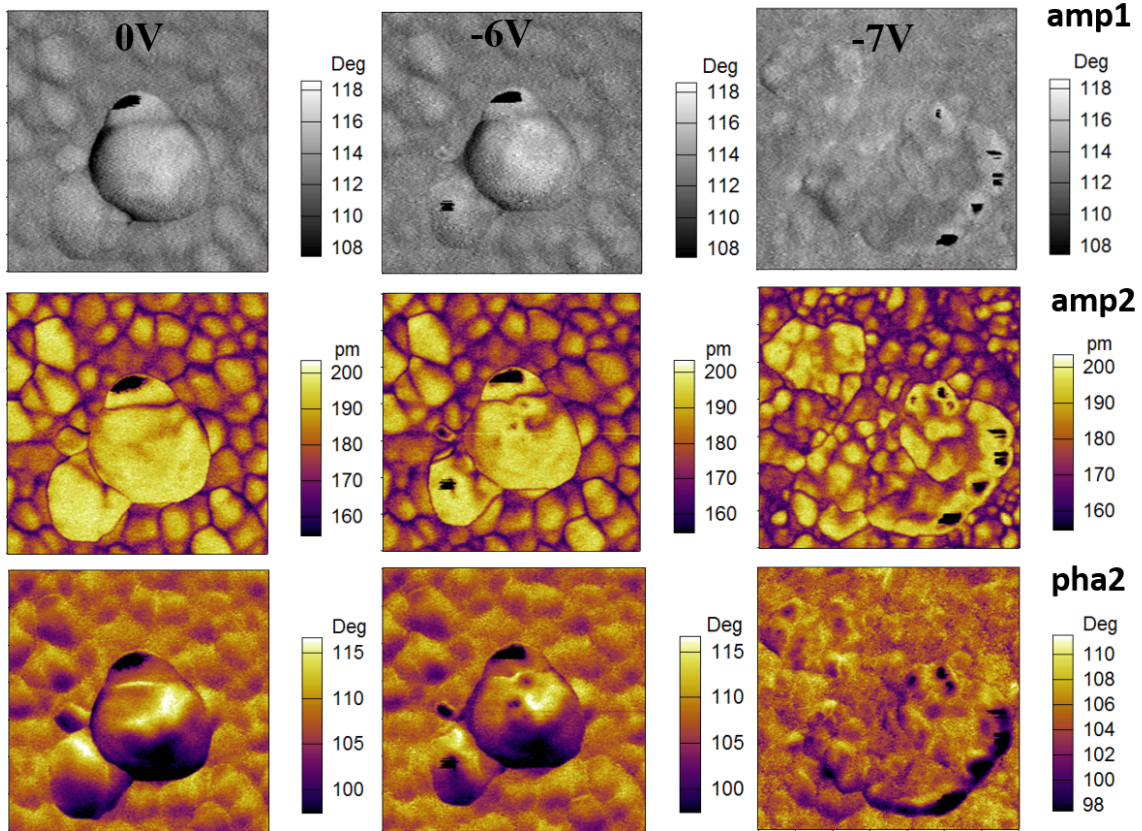
Table S2, Specifications of a typical SPM probe (AC240TM, Olympus, Japan) used in this work, calibrated by using the GetReal^{TM} software developed by Asylum Research (USA).

1st eigenmode resonance frequency, kHz	68.45
2nd eigenmode resonance frequency, kHz	399.95
3rd eigenmode resonance frequency, kHz	1057
1st eigenmode InvOLS$^{a)}$, nm/V	77.09
2nd eigenmode InvOLS, nm/V	28.26
3rd eigenmode InvOLS, nm/V	28.51
1st eigenmode stiffness k, N/m	1.8
2nd eigenmode stiffness k, N/m	53.56
3rd eigenmode stiffness k, N/m	319.64
1st eigenmode Q	160.1
2nd eigenmode Q	414.8
3rd eigenmode Q	611.7
Tip radius of curvature, nm	20
Cantilever dimension (L, W, H), μm	240, 40, 2.3
Tip coating, nm	Ti/Pt (5/20)
Nominal stiffness, N/m	2

$^{a)}$InvOLS: inverse optical lever sensitivity

References

1.   M. M. Thackeray, S.-H. Kang, C. S. Johnson, J. T. Vaughey, R. Benedek, S. A. Hackney, *J. Mater. Chem.* **2007**, *17*, 3112.

2.   D. C. Hurley, in *Applied Scanning Probe Methods XI: Scanning Probe Microscopy Techniques*, Vol. XI (Eds: B. Bhushan, H. Fuchs), Springer, Heidelberg **2009**, 97.